International Journal of Mass Spectrometry and Ion Processes, 104 (1991) 179–211
Elsevier Science Publishers B.V., Amsterdam

CHARGE-REMOTE FRAGMENTATION OF GAS-PHASE IONS: MECHANISTIC AND ENERGETIC CONSIDERATIONS IN THE DISSOCIATION OF LONG-CHAIN FUNCTIONALIZED ALKANES AND ALKENES

VICKI H. WYSOCKI * and MARK M. ROSS

Chemistry Division, Naval Research Laboratory, Washington, DC 20375-5000 (U.S.A.)

(First received 14 May 1990; in final form 7 September 1990)

ABSTRACT

The collision-activated dissociation pathways of a number of long-chain functionalized alkane ions, $CH_3(CH_2)_nX^+$, and alkene ions have been examined by tandem mass spectrometry. Major dissociation pathways observed following collisional activation include the loss of C_nH_{2n+2} units, the loss of C_nH_{2n+1} units, the formation of $C_nH_{2n+1}^+$, and the formation of X^+ or XH^+. Isotopic labelling data for $[(CD_3)_3N(CD_2)_{13}CH_3]^+$ show that no hydrogen/deuterium scrambling occurs between the charge site and the terminal methyl group for the losses of C_nH_{2n+2} or C_nH_{2n+1} from $[(CH_3)_3N(CH_2)_{13}CH_3]^+$. The collision energy required to detect charge-remote fragmentation in low-energy (electronvolt) collisional activation experiments was found to vary with compound type, ion formation method, mass of collision target, and target gas pressure. It is proposed that the dependence of the product distribution on the type of compound is caused by competition between charge-remote fragmentation and charge-directed processes such as the formation of $C_nH_{2n+1}^+$ or the formation of X^+ or XH^+. A radical mechanism is proposed to account for several charge-remote dissociation pathways that cannot be accounted for by a previously proposed cyclic elimination mechanism. These processes include the loss of methane, the formation of odd- and even-electron product ions separated by 1 u, and the enhancement of certain dissociation products (e.g., allylic cleavage product ions) when unsaturation or substituent sites are introduced into the molecule.

INTRODUCTION

Unimolecular decompositions of excited gas-phase ions have been the subject of extensive investigation because they are fundamentally important (e.g., in studies of dissociation dynamics or of energy deposition and redistribution) and analytically useful (e.g., for structural characterization of complex molecules by mass spectrometry) [1–5]. The unimolecular dissocia-

---

* National Research Council Postdoctoral Research Associate. Present address: Department of Chemistry, Virginia Commonwealth University, Richmond, VA 23284-2006, U.S.A.

tion of large ions is currently of special interest since (i) it is now possible to produce gaseous ions from samples that previously were not amenable to analysis by mass spectrometry, and (ii) the structural characterization of polymers and biomolecules depends on the development of a base of knowledge concerning the energetics and mechanisms of dissociation of large energized ions. An unusual type of unimolecular dissociation, termed remote-site or charge-remote fragmentation, has been proposed to occur without the involvement of the charge site of large even-electron ions [6,7]. This is in contrast to most conventional ionic fragmentation mechanisms which involve the charge and/or radical sites of the ion [3,4].

Charge-remote fragmentation was noted by Gross and co-workers [6–14] in a series of ion structural investigations which utilized tandem mass spectrometry. Ions of interest were produced by fast-atom bombardment (FAB), mass selected and allowed to undergo collisions at 8 keV (laboratory energy) with helium target atoms. An electric sector scan was used to analyze fragment ions, producing spectra consisting of broad peaks 14 u apart. The extensive investigations of Gross and co-workers have shown that this type of fragmentation occurs for a wide variety of compound classes including (i) carboxylate, alkylsulfate, steroid, and alkylsulfonate anions, (ii) alkylammonium and alkylphosphonium cations, (iii) protonated alkyl amines, amides, carboxylic acid pyrrolidides, and picolynyl esters, and (iv) lithiated fatty alcohols, acids and esters [6–14]. In addition to the publications of Gross and co-workers, other examples of decompositions which formally occur remote to the charge site have been reported but the dissociations often have not been identified as such [15–21].

The major series of charge-remote fragment ions reported for positive or negative ions of various functionalized alkanes $CH_3(CH_2)_nX^+$ (where X is a functional group) corresponds to the loss of C_nH_{2n+2} units upon collisional activation [6–14]. It has been shown that if the terminal hydrogen (H) of a structure such as $HCH_2(C_nH_{2n})X^+$ is replaced by another group (Y) to produce $YCH_2(C_nH_{2n})X^+$, units of $C_nH_{2n+1}Y$ are lost with no scrambling between Y and the charge site [7]. If an unsaturation site is introduced into a molecule, fragmentation is suppressed, although not eliminated, at vinylic positions and positions corresponding to cleavage of the double bond. This behavior, and production of characteristic fragmentation patterns for compounds containing substituent sites, makes charge-remote fragmentation useful for determinations of chain length and locations of unsaturation or substituent sites [7,9,10,13]. The 1,4-cyclic elimination mechanism:

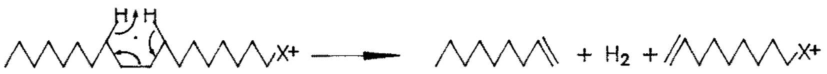

(1)

was proposed [7] because it is consistent with all of these observations and also with the fragmentation patterns observed when an unsaturated compound is deuterated across the double bond and then collisionally activated. However, this mechanism does not account for the observed loss of CH_4 from $CH_3(CH_2)_nX^{+/-}$ or for the enhanced relative abundance [9,12] of ions corresponding to cleavage allylic to a double bond.

Publications on charge-remote dissociation have focussed on surveying the types of compounds that undergo the fragmentation, the analytical utility of the fragmentation, and the mechanism and energetics of the fragmentation. Most of these investigations used high-energy collisional activation with an electric sector scan to analyze product ions. The results of these studies lead to our interest in fundamental aspects of charge-remote fragmentation and we have focussed on two areas. Firstly, the loss of C_nH_{2n+2} has been the major charge-remote fragmentation pathway considered. However, methods that provide unit resolution of product ions have indicated that C_nH_{2n+1} loss may also occur [17,22,23]. It is of interest to determine whether this ion series also occurs without the direct involvement of the charge site. Secondly, it has been reported [6–14] that charge-remote fragmentation by loss of C_nH_{2n+2} generally is not observed in a conventional FAB mass spectrum but that it occurs upon collisional activation in the kiloelectronvolt (high-energy) regime. High-energy collisional activation results in deposition of a broad distribution [24–28] of internal energy into the ion population and this can make difficult the elucidation of the energetics of dissociation. The use of other methods, such as low-energy collision-activated dissociation may provide additional information on the energy requirements and mechanism of the reaction, as suggested by our preliminary investigation [22]. Prior to the present work, laboratory collision energy onsets for charge-remote fragmentation of < 30 eV [22], 175 eV [11], 200–300 eV [18], 400 eV [29], or > 1 keV [7,12] have been reported. The data presented in this paper show that relative abundances of charge-remote fragment ions are quite sensitive to compound type, collision energy, mass of the collision gas, and collision gas pressure and help to explain the earlier seemingly contradictory reports.

We report here low-energy (0–195 eV laboratory collision energies) and high-energy (kiloelectronvolt laboratory collision energies) collisional activation data which provide information on the mechanisms and energetics of fragmentation of ionized long-chain functionalized alkanes and alkenes (for a preliminary communication see ref. 30). For compounds of the general type $CH_3(CH_2)_nX^+$, major dissociation pathways were found to include loss of C_nH_{2n+2}, loss of C_nH_{2n+1}, formation of $C_nH_{2n+1}^+$, and formation of X^+ or XH^+. The goals of the research are to determine (i) whether charge-remote loss of C_nH_{2n+2} occurs at collision energies in the electronvolt range for the compounds investigated, (ii) whether the internal energy content of the ions prior to collisional activation affects their collision-activated dissociation patterns, (iii) whether any competitive dissociations that occur may be classified as charge-remote fragmentation, (iv) the energetics of C_nH_{2n+2} loss relative to the energetics of the other dissociation pathways, and (v) if any of the competitive dissociation pathways are related mechanistically. To address these issues, the internal energy of a variety of different compounds was systematically varied under conditions that provide unit mass resolution of the fragment ions. The influence of factors such as the precursor ion internal energy, ion kinetic energy, ion size (number of degrees of freedom), time frame of reaction, type of functional group present and the kinetics of competing reactions were considered.

RESULTS

Tanden mass spectrometry (MS–MS) [2,4,5], a proven technique for the study of unimolecular dissociation characteristics, was utilized in this investigation of the dissociation patterns of a series of even-electron ions. A typical MS–MS experiment includes (i) generation and mass selection of the ionic species of interest, (ii) activation to induce dissociation, and (iii) mass analysis of the resulting fragment ions. When a collection of ions is generated and activated in a tandem mass spectrometry experiment, transitions to various electronic, vibrational, and rotational states of the ions are possible, leading to a collection of excited ions with a distribution of internal energies. For polyatomic molecules, rapid conversion of energy is believed to precede fragmentation, which usually occurs from high vibrational levels of the ground electronic state [3]. The ions dissociate unimolecularly to produce a spectrum that is dependent on the activation energy for each fragmentation reaction, the relative rates of the reactions, the time available for reaction, and the distribution of internal energies of the ions. The use of mass spectral data to investigate the energetics and mechanism of a dissociation reaction requires consideration of all these factors.

A common means of investigating the energetics and mechanism of a reaction is to vary systematically the internal energy of the reactant molecules. In our study, gas-phase ions were generated by chemical ionization [31] or FAB [32] of the organic sample molecules. The parent ion of interest was activated, after mass selection, by collision with neutral gas-phase targets in either the high- (kiloelectronvolt) or low-energy (electronvolt) range of laboratory ion kinetic energies [2,5]. For low-energy collisional activation experiments, a variety of experimental conditions that result in deposition of different amounts of internal energy into the ions were utilized. These include

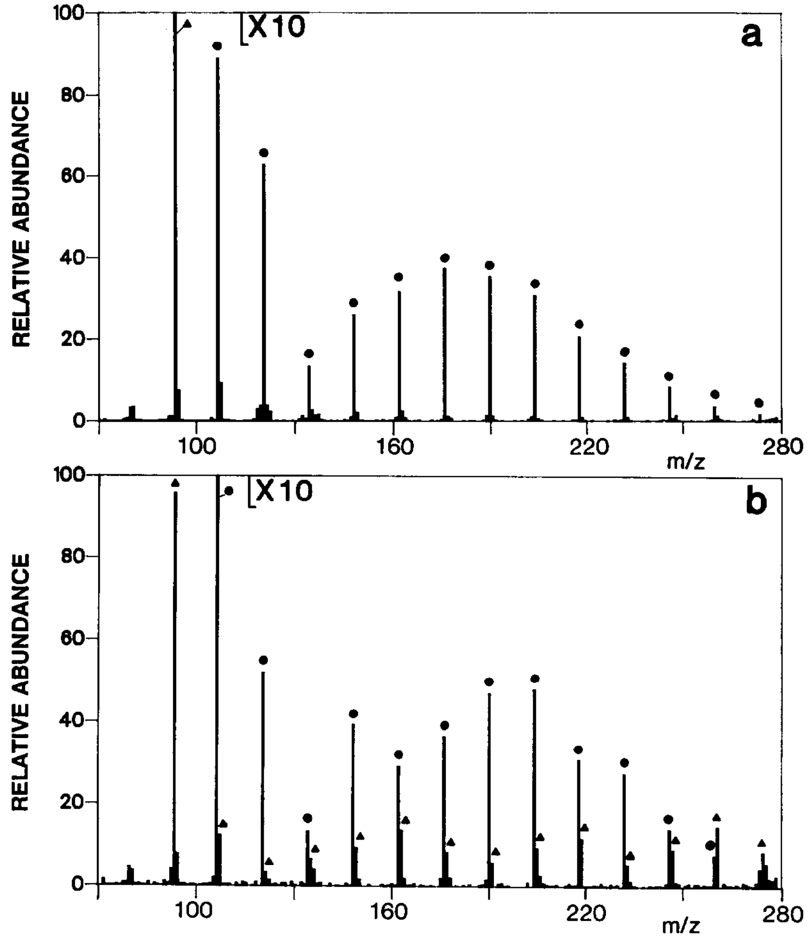

Fig. 1. Illustration of the influence of the ion production method on the collision-activated dissociation spectra of protonated 4-pentadecylpyridine. Ions were generated by (a) FAB or (b) isobutane CI. Mass-selected parent ions (*m/z* 290) were activated by a 150 eV collision with O_2 target (0.06 mTorr, $E_{cm} = 15$ eV; Ar gives same results). Triangles represent losses of C_nH_{2n+1}; circles represent losses of C_nH_{2n+2}.

variation of (i) the ion generation conditions, (ii) the collision energy, (iii) the mass of the target gas, and (iv) the pressure of the target gas.

Low-energy collisional activation

Precursor ion internal energy

Fast-atom bombardment is the ion production method that has been utilized in the majority of previous investigations. We used two methods in attempts to produce ions of lower internal energies than those produced by

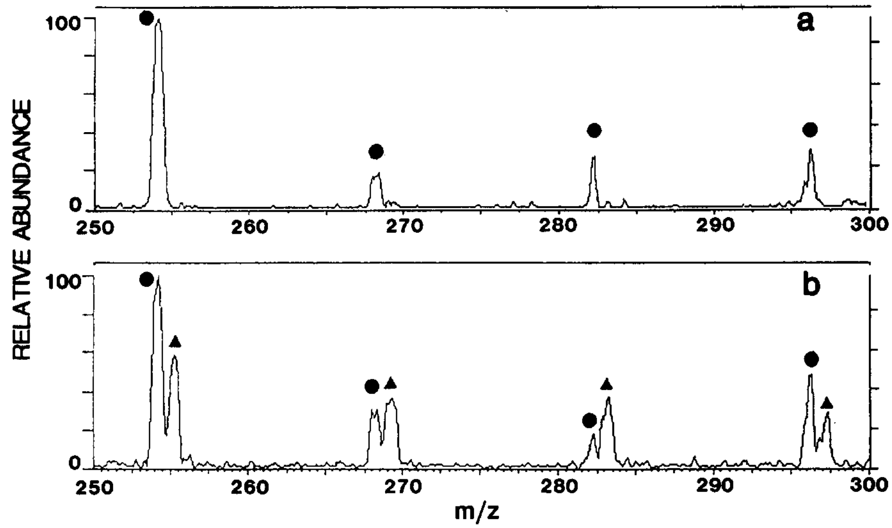

Fig. 2. Illustration of the influence of the ion production method on the collision-activated dissociation spectra of trimethyloctadecylammonium ions, $[(CH_3)_3N(CH_2)_{17}CH_3]^+$. Ions were generated by (a) FAB, or (b) HP-FAB. Mass-selected parent ions (*m/z* 312) were activated by a 100 eV collision with Xe target at a pressure of 0.06 mTorr (E_{cm} = 30 eV). Triangles represent losses of C_nH_{2n+1}; circles represent losses of C_nH_{2n+2}.

standard FAB. These were (i) chemical ionization (CI) [31], in which the internal energy of the ions is determined by the exothermicity of the protonation reaction followed by collisional cooling of the ions in the high pressure of reagent gas present [27], and (ii) high-pressure-fast-atom bombardment (HP-FAB) [33] in which FAB is performed in the presence of a high pressure of bath gas to collisionally cool the ions.

The data show that the method used to prepare ions prior to collisional activation in the electronvolt energy range affects the overall fragmentation pattern detected following low-energy collisional activation. This is illustrated in Figs. 1 and 2, which show low-energy collisional activation spectra obtained with a quadrupole mass analyzer. This quadrupole analyzer provides unit mass resolution of the fragment ions (product ions formed following collision of the mass-selected ion). The spectra show that ions produced by chemical ionization or HP-FAB dissociate upon collisional activation in the electronvolt energy range by loss of alkyl radicals ($-C_nH_{2n+1}$) in addition to loss of C_nH_{2n+2} while the corresponding ions produced by standard FAB show little loss of C_nH_{2n+1}. The C_nH_{2n+1} loss ions may initially be distonic radical ions, $^{\cdot}CH_2(CH_2)_nX^+$ [34,35].

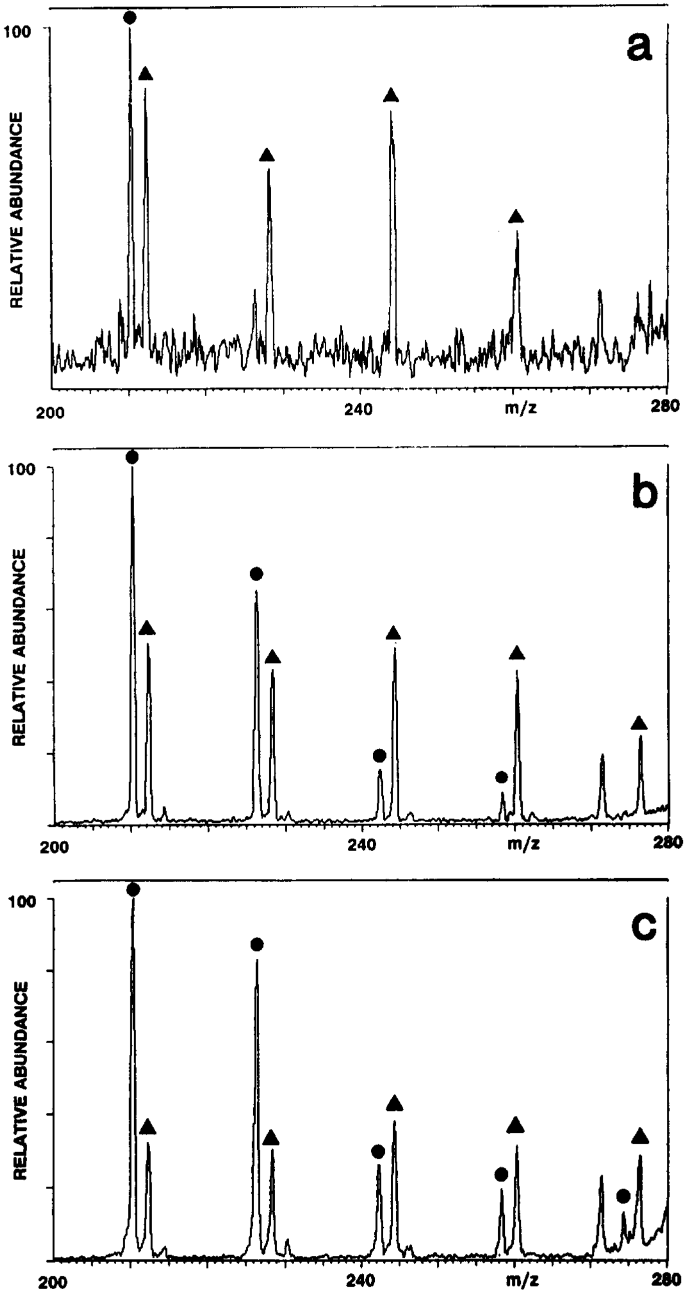

Fig. 3. Collision-activated dissociation spectra of $[(CD_3)_3N(CD_2)_{13}CH_3]^+$, produced by HP-FAB, activated by laboratory collision energies of (a) 50 eV, (b) 100 eV and (c) 190 eV with Xe (single collision conditions). The corresponding center-of-mass energies are (a) 16 eV, (b) 31 eV, and (c) 59 eV. Triangles mark peaks corresponding to loss of alkyl radicals $(-C_nD_{2n-2}H_3)$; circles mark peaks corresponding to loss of $C_nD_{2n-1}H_3$. For an unlabelled compound these losses correspond to the losses of C_nH_{2n+1} and C_nH_{2n+2}, respectively.

TABLE 1

Ions that were mass-selected and collisionally activated to investigate the energetics and mechanism of charge-remote fragmentation; maximum internal energy, center-of-mass energy (E_{cm}), available upon collision of each of the ions with Xe is given for laboratory collision energies of 10 and 195 eV

	E_{cm} (eV)	
	E_{lab} = 10 eV	E_{lab} = 195 eV
$CH_3(CH_2)_{17}NH_3^+$	3	64
$CH_3(CH_2)_7CH{=}CH(CH_2)_8NH_3^+$	3	64
$[CH_3(CH_2)_{17}]N^+[CH_3]_3$	3	58
$[CH_3(CH_2)_{17}]_2N^+[CH_3]_2$	2	38
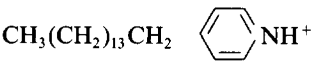	3	61
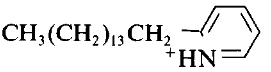	3	61
$CH_3(CH_2)_7CH{=}CH(CH_2)_8OHLi^+$	3	63
$CH_3(CH_2)_7CH{=}CH(CH_2)_8OH_2^+$	3	64

Deuterium labelling results for $[(CD_3)_3N(CD_2)_{13}CH_3]^+$ illustrate that neither the loss of C_nH_{2n+1} nor the loss of C_nH_{2n+2} involves hydrogen scrambling between the remote alkyl terminus and the charge site. This is illustrated in Fig. 3 which shows that both series of losses ($-C_nH_{2n+1}$ and $-C_nH_{2n+2}$) are always observed with loss of all three hydrogens of the unlabelled terminal methyl group of the long alkyl chain [36].* For the labelled compound, these series correspond to loss of $C_nD_{2n-2}H_3$ and loss of $C_nD_{2n-1}H_3$. A series of ions of low relative abundance, corresponding to loss of C_nH_{2n} for unlabelled compounds, is visible in Fig. 3; these losses also occur without hydrogen scrambling.

---

* Note that for the deuterated tetraalkylammonium ion, $[(CD_3)_3N(CD_2)_{13}CH_3]^+$, any alkyl ions containing all D can overlap with the $C_nD_{2n-1}H_3$ loss series; they appear at the same nominal mass. However, this is not a serious problem and does not compromise the data shown in Fig. 3. For the highest members of the series, those shown in Fig. 3, there is no overlap possible. The highest mass all-deuterium alkyl ion theoretically possible is $C_{12}D_{25}^+$, *m/z* 194 from $C_{14}D_{26}H_3^+$ via the mechanistically implausible loss of C_2H_3D. We know from our data and data in the literature for the unlabelled compound that the alkyl ion series extends in significant abundance only out to 6 carbons [36]. That is, while the *m/z* 98 ion may be composed of both an alkyl ion contribution and a contribution from loss of $C_nD_{2n-1}H_3$, intermediate members of the series are composed almost entirely of loss of C_nH_{2n+2} and the highest members (> *m/z* 200) can only be caused by loss of $C_nD_{2n-1}H_3$.

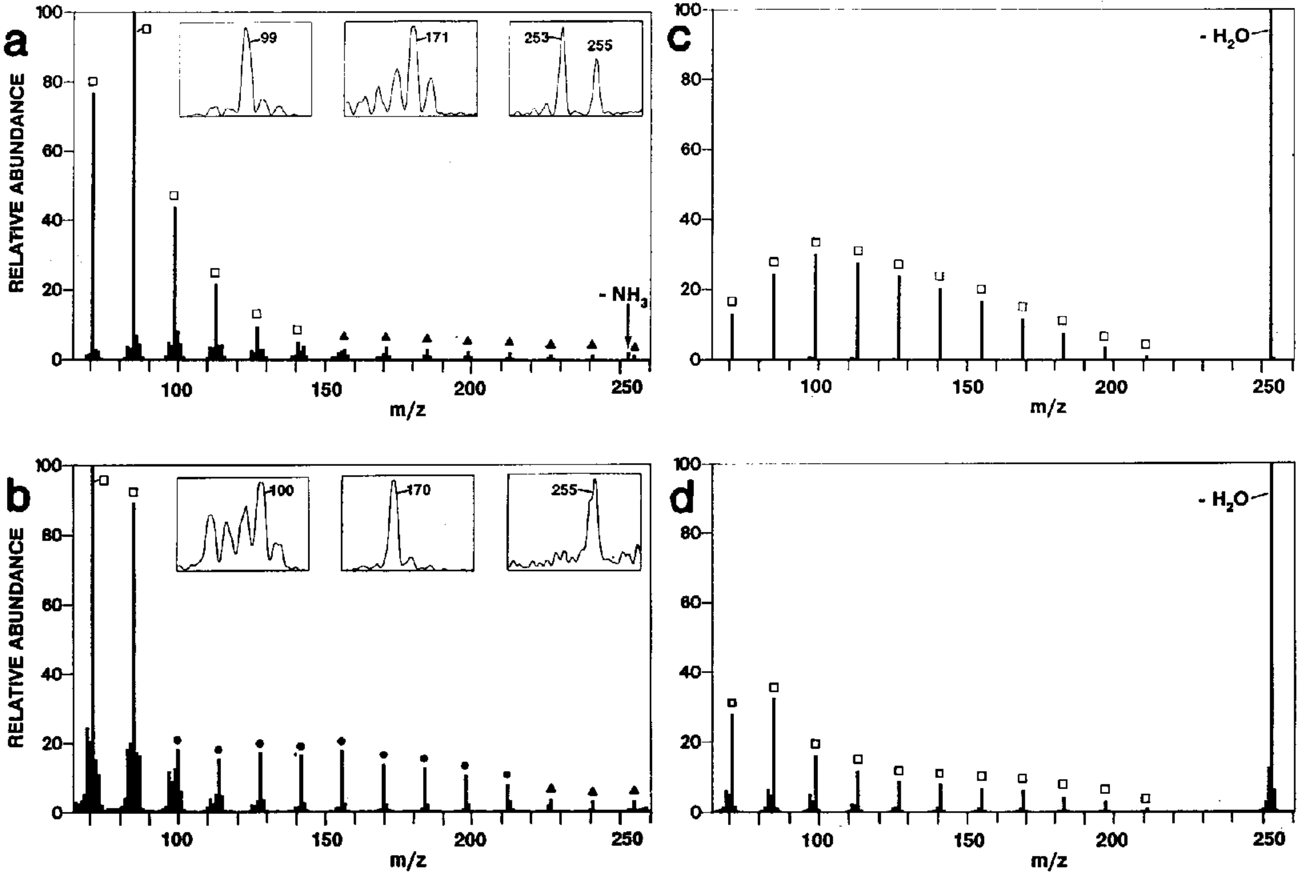

Fig. 4. Collision-activated dissociation spectra of protonated *n*-octadecylamine at (a) 10 and (b) 150 eV laboratory collision energies and protonated *n*-octadecylalcohol at (c) 10 and (d) 150 eV laboratory collision energies (0.07 mTorr Xe target gas; ions produced by isobutane CI). The corresponding E_{cm} values are (a) 3 eV, (b) 49 eV, (c) 3 eV, and (d) 49 eV. Triangles mark peaks corresponding to loss of alkyl radicals ($-C_nH_{2n+1}$), circles mark peaks corresponding to loss of C_nH_{2n+2}, and squares mark peaks corresponding to alkyl ions, $C_n^+H_{2n+1}^+$. Peak profile data are shown in the insets of (a) and (b) for the mass ranges 95–103, 167–175, and 250–258.

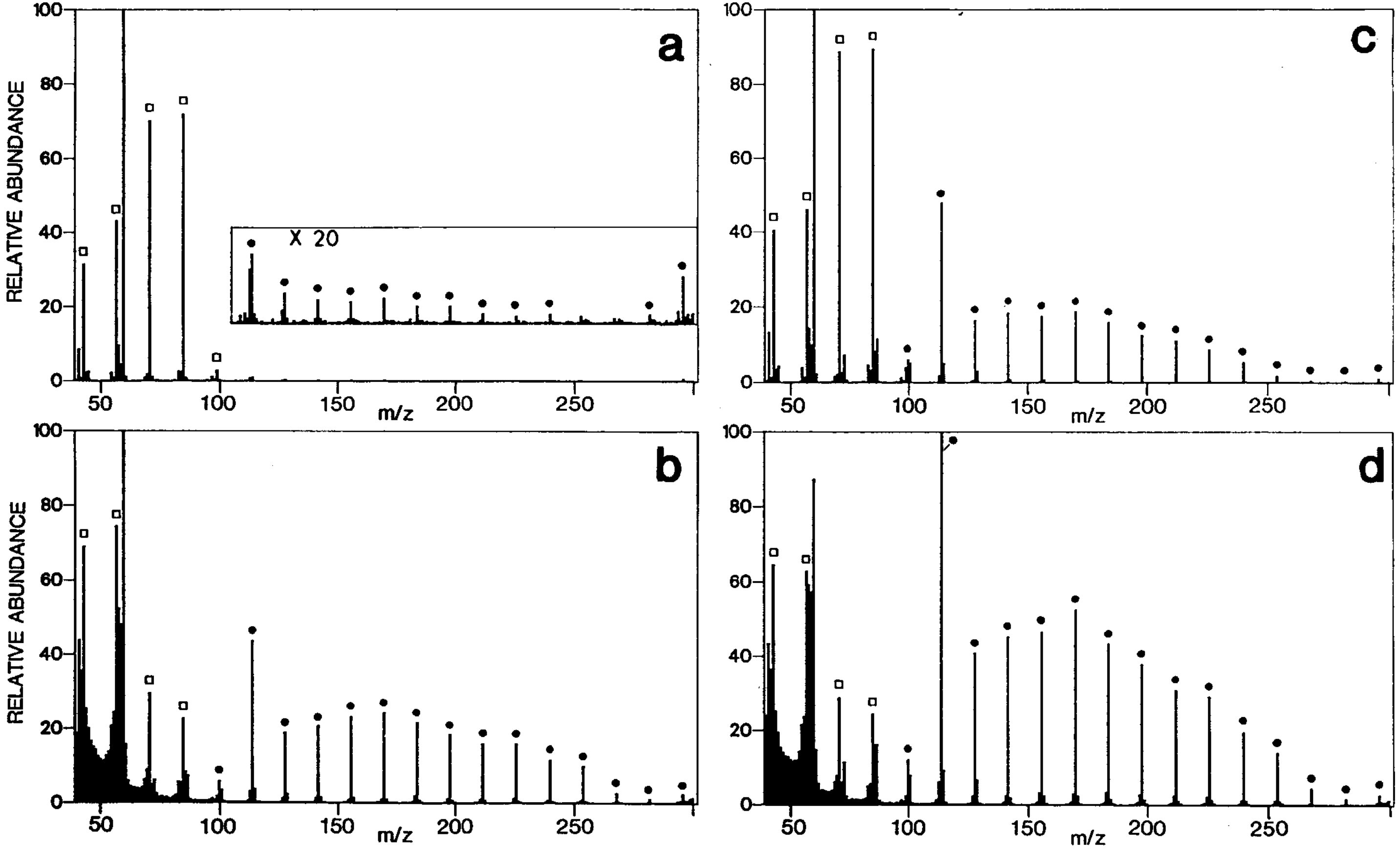

Fig. 5. Collision-activated dissociation fragment ion spectra of FAB-generated trimethyloctadecylammonium ions. Spectra were obtained at collision energies of (a) 50 eV and (b) 195 eV with Ar (0.06 mTorr) and (c) 50 eV and (d) 195 eV with Xe (0.07 mTorr). The corresponding E_{cm} values are (a) 6 eV, (b) 22 eV, (c) 15 eV, and (d) 58 eV. Circles represent losses of C_nH_{2n+2}; squares represent alkyl ions, $C_nH_{2n+1}^+$.

Variation of ion kinetic energy

Each of the ions listed in Table 1 was mass-selected and allowed to undergo collisional activation at energies in the range of 0–195 eV under single collision conditions. Figures 4 and 5 illustrate the strong influence that the compound type and collision energy can have on the fragmentation pathways observed.

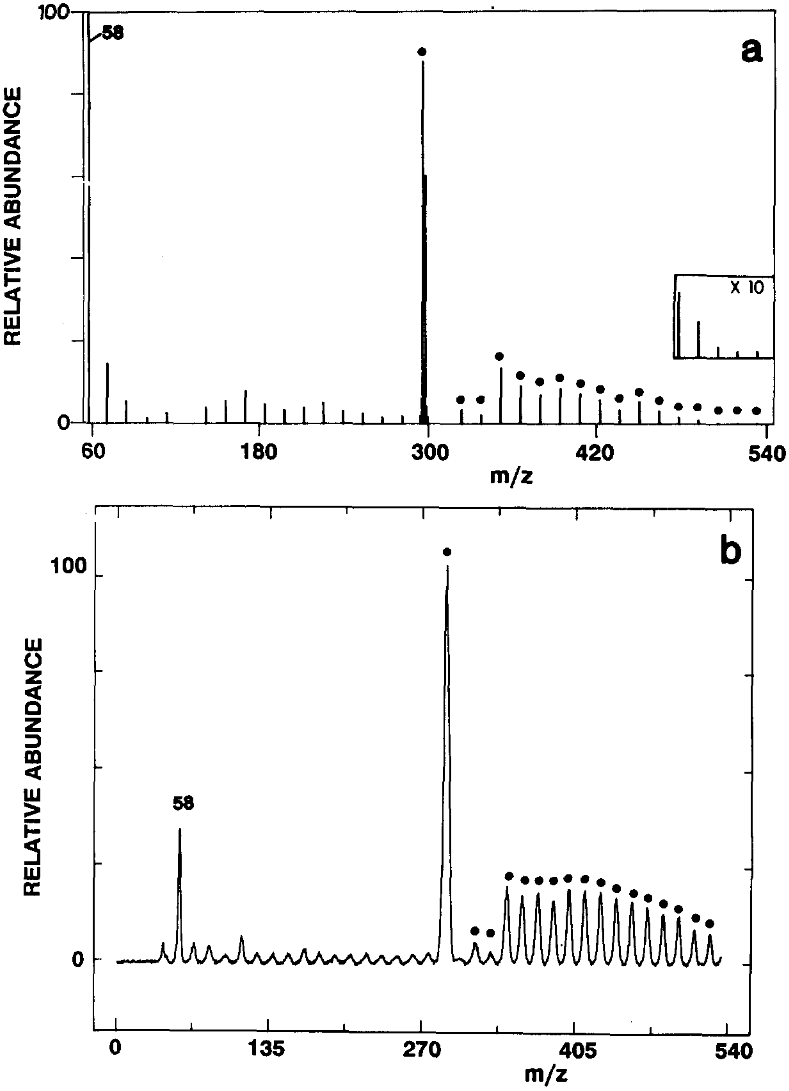

Fig. 6. Collision-activated dissociation spectra of FAB-generated dimethyldioctadecylammonium ions. Spectra were acquired by using laboratory collision energies of (a) 190 eV with Xe (triple quadrupole instrument; $E_{cm} = 37$ eV), and (b) 8000 eV collisions with He (sector instrument, $E_{cm} = 58$ eV; kinetic energy release results in broad peaks when an electric sector is used for the final stage of analysis). Circles represent losses of C_nH_{2n+2}.

Comparison is appropriately made for three ions of similar mass and similar numbers of degrees of freedom: protonated octadecylammonium ion (*m/z* 270), protonated octadecylalcohol (*m/z* 271), and trimethyloctadecylammonium ion (*m/z* 312). Alkyl ions, thought to be produced by an initial charge-directed loss of a small neutral molecule (e.g. NH_3, H_2O, $(CH_3)_3N$) followed by loss of alkenes from the resulting carbocation [7,13,37,38], are present in the CAD spectra of all three compounds, but only the spectra of the amines show the charge-remote loss of C_nH_{2n+2}. Under identical reaction conditions (cf. Figs. 4b, 4d, 5d; 195 eV single collisions with Xe), different extents of charge-remote loss of C_nH_{2n+2} are observed for the three compounds. In addition to the ion series described above, we also observed low mass ions produced by a direct bond cleavage or rearrangement at the charge site.* Examples include NH_4^+ from the protonated primary amines; Li^+ and $LiOH_2^+$ from lithiated oleyl alcohol; $C_5NH_5^+$ from the protonated alkylpyridines; and R_3NH^+ from the quaternary ammonium ions.

Charge-remote loss of C_nH_{2n+2} was detected upon collisions in the low-energy (electronvolt) range for all the compounds of Table 1 except the protonated alcohol, which also does not undergo the dissociation reaction upon high-energy [12] collisional activation. In collisional activation experiments in the electronvolt energy range, the results obtained by systematically varying the laboratory collision energy provide information on the internal energy required for fragmentation. In general, the relative abundance of ions formed by loss of C_nH_{2n+2} increased with increasing collision energy (single collision conditions) over the entire collision energy range available (0–195 eV). The spectra obtained at the higher end of this low-energy collisional activation range can be strikingly similar to 8 keV spectra. This is illustrated for dimethyldioctadecylammonium ion in Fig. 6, which compares spectra obtained upon 195 eV collision with Xe (single collision conditions) and 8 keV collisions with He. The lowest energy at which the losses of C_nH_{2n+2} could be detected varied significantly from compound to compound. This holds true for both the laboratory and the center-of-mass frame of reference. The maximum internal energy available upon a 10 or 195 eV collision of Xe with each of the molecules is listed in Table 1; this is the center-of-mass energy,

---

* In Fig. 5, the enhanced abundance of the ion of *m/z* 114, relative to its neighbors 14 u higher and lower in mass, can be explained by a contribution from another fragmentation pathway recently identified by Tuinman et al. [39]. Their data for various labelled compounds show that there is a contribution to the C_nH_{2n+2} loss series from ions that have lost part of the alkyl chain plus one of the methyl groups from the nitrogen. This contribution is greatest for the ion of *m/z* 114 with minor contributions to higher mass ions.

E_{cm}.* The lowest E_{cm} at which loss of C_nH_{2n+2} could be detected varied from 1 eV to greater than 10 eV in the order pentadecylpyridine < lithiated oleyl alcohol < alkylammonium ions, with no loss detected for protonated octadecylalcohol. The lowest laboratory collision energy at which charge-remote loss of C_nH_{2n+2} could be detected also varied with the ion formation method. For example, ions that were collisionally cooled during HP-FAB required higher collision energies to promote loss of C_nH_{2n+2} than did those that were formed in normal FAB conditions.

The spectra reveal that the relative abundances of the ions formed by loss of alkyl radicals (C_nH_{2n+1}) and the loss of C_nH_{2n+2} vary with laboratory collision energy. That is, the ratio of products of C_nH_{2n+1} loss to the corresponding products of C_nH_{2n+2} loss decreases (for a given value of *n*) with increasing collision energy (see Figs. 3 and 4). These data agree with the results of variation of precursor ion internal energy (see above). The relative abundances of charge-directed fragmentation products in the collisional activation spectra also vary with the ion formation method. For example, the higher members of the series of alkyl ions (e.g., 43^+, 57^+, 71^+, 95^+,...) are of greater relative abundance in the collisional activation spectra when the ion generation method is CI or HP-FAB instead of normal FAB.**

In order to investigate these fragmentations over a different time window than that available in the quadrupole and sector instruments, low-energy collisional activation data were obtained on a Fourier transform ion cyclotron resonance instrument (FTMS) [40] for 2-pentadecylpyridine and for protonated octadecylamine. This extends the time scale for fragmentation to

---

* For collisional activation experiments performed under conditions in which each ion undergoes no more than one collision, the maximum internal energy available by conversion of laboratory collision energy, E_{lab} into internal energy can be calculated by converting to the center-of-mass frame of reference. The center-of-mass energy is given by $E_{cm} = E_{lab}[m_t/(m_t + m_i)]$, where *m* and m_i are the masses of the neutral target gas and the projectile ion, respectively. Note that this is the maximum energy available and that the actual ion population will contain a range of internal energies with the most probable energy deposited being less than the maximum available.

**The greater abundance of $C_nH_{2n+1}^+$ ions (of high *n* values) for protonated alcohols versus protonated amines has been suggested, for chemical ionization spectra, to be due to incomplete randomization of internal energy through all the vibrational modes of the [RXH^+] species prior to rupture of the R^+–XH bond [38]. Because we see the same fragmentation trends upon CAD, we suggest that the difference is actually due to the differing proton affinities of NH_3 and H_2O versus an alkene (the conjugate base of R^+). That is, amines of low internal energy may lose NH_3 as an ammonium ion (NH_4^+). All alkyl ions are then products of dissociation of amines of high internal energy which have fragmented directly to NH_3 and an alkyl ion (extensive fragmentation, only alkyl ions of low *n* values detected). For protonated alcohols, H_2O is lost directly as a neutral from ions of all internal energies because of its relatively low proton affinity; alkyl ions corresponding to a range of *n* values are detected. This will be discussed in more detail elsewhere.

milliseconds rather than microseconds. The pentadecylpyridine ion showed charge-remote loss of C_nH_{2n+2} over a range of collision energies, including the lowest laboratory collision energy attempted (4 eV, Xe), in agreement with published FTMS data for 4-pentadecylpyridine which showed the fragmentation over a range of collision energies from 2.5 to 860 eV [41]. Protonated octadecylamine fragmented only by formation of alkyl ions; no losses of C_nH_{2n+2} or C_nH_{2n+1} were detected.

Mass of collision target

Another means of varying the internal energy deposited by low-energy collisional activation is to use collision targets of different masses [42]. Argon and xenon were used as collision targets for this study. In our experiments, the more massive target Xe was more effective in promoting greater relative abundances of charge-remote fragmentation than was Ar at the same laboratory collision energy.* This is illustrated for trimethyloctadecylammonium ion in Fig. 5 which shows spectra obtained under single collision conditions. Note that it has been previously reported, in studies of accurate threshold measurements by low-energy collisional activation, that dissociation with Xe appears to be more efficient than that observed with Ar even at the same center-of-mass energy [44]. This is thought to be due to the higher polarizability and longer interaction time for Xe as compared to Ar.

Pressure of target gas

An additional way to vary internal energy deposition in low-energy collisional activation is to increase the pressure of the target gas [45]. This method has two major problems associated with it for fundamental studies: ions may isomerize between collisions and initially formed fragment ions may themselves undergo collisions and fragment further. The fragmentation of several of the compounds listed in Table 1 was investigated as a function of collision gas pressure. In some cases, high collision gas pressures were not advantageous for production of the complete series of charge-remote fragment ions (all *n* values) because higher mass ions decreased in abundance, or disappeared, with increasing collision gas pressures. The ratio of products of C_nH_{2n+1} loss to products of C_nH_{2n+2} loss was found to decrease (for a given value of *n*) with increasing collision gas pressure, as it did with increasing collision energy.

---

* This difference may go undetected when the mass of the target is large compared to that of the projectile ion: significant ion loss may be caused by scattering of the fragments beyond the acceptance angle of the mass spectrometer (see ref. 43).

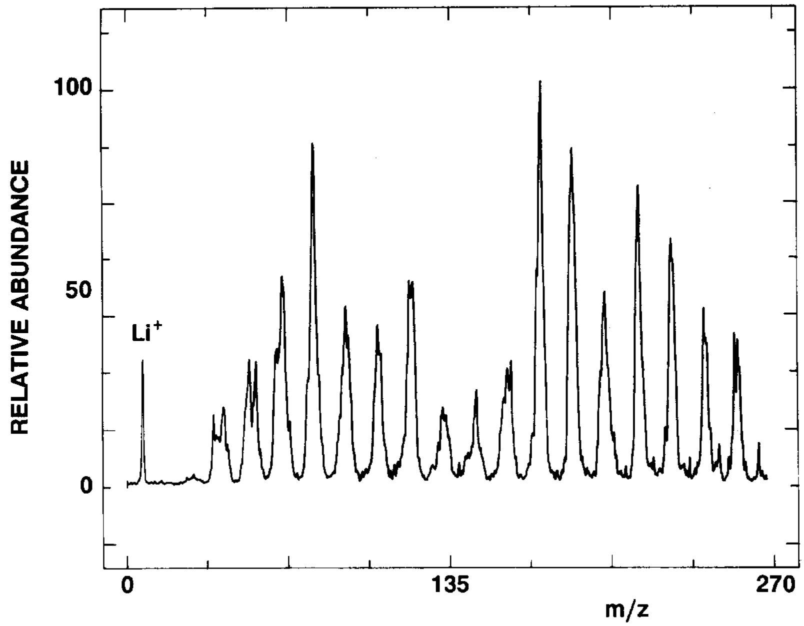

Fig. 7. High-energy (8000 eV, He target) collision-activated dissociation spectrum of lithiated oleyl alcohol. A conversion dynode voltage of 10 kV was used to improve detection of the lithium ion (normal setting, 5 kV).

High-energy collisional activation

Charge-remote fragmentation has been reported previously for collisional activation in the kiloelectronvolt range for most of the compound classes examined here [7,12,13,46]. Selected compounds were investigated in this energy regime for comparison purposes. All of the compounds of Table 1 that undergo charge-remote fragmentation also fragment by charge-directed routes upon collisional activation in both the electronvolt and kiloelectronvolt ranges. In contrast to a literature report [12], results from our laboratory indicate that lithium ion is produced, in addition to charge-remote loss of C_nH_{2n+2}, upon 8 keV collisional activation of lithiated oleyl alcohol (Fig. 7). There are significant detection and collection efficiency problems which probably account for the literature results. These problems are associated with the low kinetic energy ((7/275) × 8000 eV) of the small product ion and the consequent likelihood of scattering and low detection efficiency. These problems are expected to be particularly severe in a sector instrument where kinetic energy analysis is performed. We note that we had to increase the conversion dynode voltage to 10 kV, 5 kV above its normal setting, in order to obtain the spectrum shown here. Further experiments are required to determine the true ratio of the lithium ions to the ions corresponding to charge-remote fragmentation.

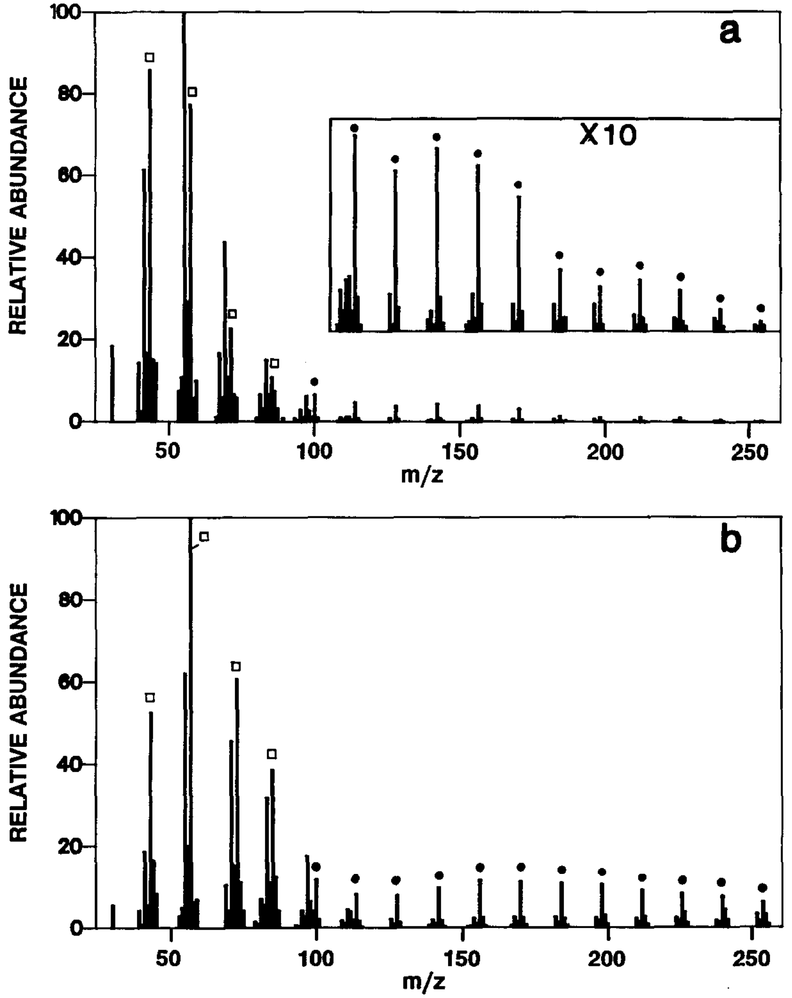

Fig. 8. Collision-activated dissociation fragment ion spectra of protonated *n*-octadecylamine obtained by (a) 3000 eV, 1.5° collisions upon Ar and (b) 3000 eV, zero angle collisions upon Ar (hybrid [BEQQ] instrument). Circles represent losses of C_nH_{2n+2}; squares represent alkyl ions, $C_nH_{2n+1}^+$.

Variation of collision energy or collision gas pressure is thought to have only limited influence on the fragmentation patterns observed upon kiloelectronvolt collisional activation [5,47]. A method used in kiloelectronvolt collisional activation to detect products of ions of different internal energies is angle-resolved mass spectrometry, in which product ions are collected as a function of scattering angle [5]. For some ions, it has been shown that relative abundances of fragment ions obtained as a function of scattering angle correlate with parent ion internal energy (following collision). One complication of this method is that the kinetic energy released in dissociation can contribute to the fragment ion angular distribution. Angle-resolved mass spectra of protonated octadecylamine (Fig. 8) and protonated 2-pentadecylpyridine indicate that charge-remote fragmentation decreases relative to charge-directed fragmentation as the collection angle increases. The relative abundances of higher mass fragment ions in the charge-remote series are influenced more than those of lower mass fragment ions. The latter trend has been noted for fatty acid anions [48].

If we assume that all the ions of a particular series, such as those corresponding to loss of C_nH_{2n+2}, have similar internal energy requirements for formation, the decreased abundance of higher mass ions at larger scattering angles may simply indicate that the more massive ions are scattered to a lesser degree than the less massive ions. In addition, if large amounts of internal energy are deposited, primary high mass product ions may undergo further fragmentation to form lower members of the series. For comparisons between series, the angle-resolved results may reflect the relative rates for dissociation and the likelihood of scattering of the fragments based on their relative masses, and not the relative critical energies for fragmentation. Although larger scattering angles are generally associated with greater energy deposition, conclusions on relative energetics of fragmentation cannot be drawn from the angle-resolved data for fragmentation products widely separated in mass.

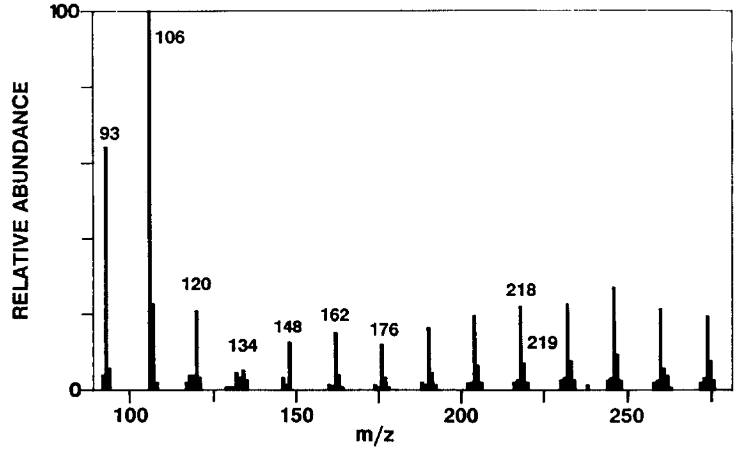

Fig. 9. Spectrum that results when protonated 2-pentadecylpyridine (*m/z* 290) undergoes 3000 eV collisions with Ar. The *m/z* 218 ion, formed by 3000 eV collisions of protonated 2-pentadecylpyridine with Ar, was dissociated by 80 eV collisions with Xe (formed ions shown in reaction 2). The *m/z* 219 ion, formed by 3000 eV collisions of protonated 2-pentadecylpyridine with Ar, was dissociated by 80 eV collisions with Xe (formed ions shown in reaction 3 in the text).

MS-MS-MS

Experiments involving three sequential stages of mass analysis, MS-MS-MS experiments, were performed in order to investigate the structures of charge-remote dissociation product ions. The spectrum that results when protonated 2-pentadecylpyridine is mass-selected and allowed to undergo collisions with He at 3 keV is shown in Fig. 9. Two of the fragment ions, *m/z* 218 and *m/z* 219, were chosen as representatives of the series corresponding to loss of C_nH_{2n+2} and loss of C_nC_{2n+1}, respectively, and two MS-MS-MS experiments were performed [30]. To perform each experiment, protonated 2-pentadecylpyridine (the parent ion) was generated and then mass-selected by the first mass analyzer. This ion was allowed to undergo collisions at 3 keV with Ar to produce a series of primary fragment ions (the daughter ions). One of the primary fragment ions was then mass-selected and allowed to undergo collisions to produce secondary fragment ions (the granddaughter ions).

When the primary fragment ion of *m/z* 218, a C_5H_{12} elimination product generated from protonated 2-pentadecylpyridine by collisions with Ar, was mass-selected and allowed to collide with Xe target gas, a series of fragment ions corresponding to loss of C_nH_{2n} was produced (reaction 2). This granddaughter spectrum closely resembles in its main features the daughter spectrum of the protonated 2-pentadecylpyridine (Fig. 9). Moreover, when the alkyl radical loss product, *m/z* 219,* was generated from the same parent ion, mass-selected and allowed to undergo collisional activation, it displayed a similar spectrum (reaction 3). The dissociation of this ion, *m/z* 219, is more facile than the dissociation of the ion of *m/z* 218** [30]. These results show that further fragmentation of a C_nH_{2n+2} loss ion and further fragmentation of a C_nH_{2n+1} loss ion can lead to the same product ion series.

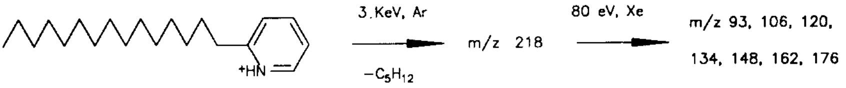

(2)

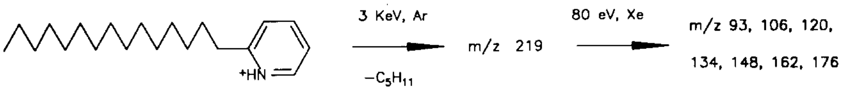

(3)

---

* Note that since a B/E linked scan was used to obtain the fragment ion spectrum of Fig. 9, there is a possibility of a contribution to the *m/z* 219 peak by C_nH_{2n+2} loss from the carbon-13 isotope (*m/z* 291) of the protonated 2-pentadecylpyridine ion. The maximum contribution possible would be 16.5% relative to the ion of *m/z* 218. Since the 219 peak is 39% of the 218 peak, at least 58% of the 219 peak [100*(39–16.5)/39] is the result of C_nH_{2n+1} loss from *m/z* 290.

**The molecular ion ($M^{+\cdot}$, *m/z* 289) of 2-pentadecylpyridine also undergoes a series of alkyl radical losses and does so with even greater facility than does the protonated molecule, with which it gives identical fragment ions.

DISCUSSION

Charge-remote loss of C_nH_{2n+2} upon low-energy (electronvolt) collisional activation

Three aspects of the energy requirements of a CAD reaction include (i) the kinetic energy frame of the ion activation step (i.e., kiloelectronvolt versus electronvolt collisions with target gas), (ii) the internal energy required to produce detectable fragment ions under given experimental conditions (e.g., a given kinetic energy and time frame), and (iii) the activation ("critical") energy required for fragmentation. Only the first of these is relatively straightforward to obtain in a mass spectrometry experiment. Attainment of (ii) from mass spectral data requires knowledge of the distribution of internal energies produced upon conversion of kinetic energy to internal energy, while attainment of (iii) requires knowledge of both the energy dependence of the rate constant for the dissociation reaction of interest and the reaction time. The internal energy content of the ions of interest following their formation but prior to collisional activation must also be considered [47,49]. This energy content, the precursor ion internal energy, is not well-characterized for molecules of the size examined here but does affect the spectra produced (see below).

The data presented here show that charge-remote loss of C_nH_{2n+2} also occurs upon collisional activation in the electronvolt range as well as at high (kiloelectronvolt) energy for many compounds.* The loss was detected upon low-energy collisional activation under single collision conditions for all the compounds of Table 1 except the protonated alcohol, which also does not undergo the dissociation reaction upon high-energy [12] collisional activation. For a compound whose dissociation energies are not known, the presence of a given fragment ion in a collisional activation spectrum at a single collision energy provides little information on the internal energy required to produce that product ion. One of the benefits of low-energy collision-activated dissociation experiments is that energy deposition varies with laboratory collision energy [5,27,44,51].** For example, spectra plotted as a function of the laboratory collision energy mimic breakdown curves which show the

---

* This observation is not surprising in view of the fact that both of these methods can deposit broad distributions of internal (vibrational) energy [24–28]. For example, the high- and low-energy collisional activation spectra of $W(CO)_6$ indicate that fragment ions with associated appearance energies ranging from 1.2 eV (for loss of a single CO) to > 17 eV (for formation of WC_2O^+) [40] are observed in both experiments (see ref. 50).

**Recently, low-energy collisional activation plots of E_{cm} versus ion abundance have been shown to give bond energies that agree very well with values measured previously by well established techniques [51]. The method has also been used to establish unknown bond energies for cluster ions [44]. Indications that internal energy increases with laboratory collision energy in the electronvolt have been extensively documented over the past decade [5,6].

internal energy dependence of mass spectra. For the lowest kinetic energy at which a given fragmentation can be observed, the maximum internal energy attainable upon collision (E_{cm}) (see Results section) plus the internal energy content of the ions prior to collision and correction for the thermal motion of the target (Doppler correction) [52] then corresponds to an upper limit of the energy required to detect the fragment ions under the given experimental conditions.

Under identical reaction conditions (cf. Figs. 4b, 4d, 5d; laboratory collision energy 195 eV, single collision with Xe), different extents of charge-remote loss of C_nH_{2n+2} are observed for different compounds. Data such as these were obtained for all the compounds of Table 1 and indicate that the lowest center-of-mass collision energy at which the compounds of Table 1 undergo charge-remote loss of C_nH_{2n+2} varies from 1 eV to $>$ 10 eV in the order pentadecylpyridine $<$ lithiated oleyl alcohol $<$ alkylammonium ions, with no loss detected for protonated octadecylalcohol. The dependence of the collision energy requirement for C_nH_{2n+2} loss on compound type was noted earlier in a study of anions and cations activated by 0–30 eV collisions with an Ar target and 0–100 eV collisions with a surface [22] and is also apparent from low-energy collisional activation experiments performed in ion cyclotron resonance mass spectrometers. For example, while FTMS data for 4-pentadecylpyridine indicate a laboratory collision energy requirement of only 2.5 eV (estimated internal energy 1.4–2.5 eV) [41] for loss of C_nH_{2n+2}, published FTMS data for n-pentyltriphenylphosphonium ions indicate a laboratory collision energy requirement of 145 eV (Ar target; E_{cm} = 15 eV) [11], and only charge-directed fragmentation (alkyl ion formation) is detected for protonated octadecylammonium ions activated at collision energies of $\leqslant$ 137 eV (Xe target; E_{cm} = 45 eV). We note here that the observation times of these three experiments vary over the range of 1–500 ms. However, our experiments in a single FTMS instrument showed that protonated 4-pentadecylpyridine fragmented by loss of C_nH_{2n+2} at energies as low as 4 eV while protonated octadecylamine did not show this loss even at the highest energy attempted (137 eV). An indication that charge-remote fragmentation is compound dependent is also given by some high-energy collisional activation data. For example, Tomer [23] has recently shown for 8 keV collision energies that charge-reversal is significantly more competitive with charge-remote fragmentations in the oleate anion than in either the octadecylsulfate or octadecylsulfonate anions.

In this discussion, we have avoided assigning values to the internal energy required for charge-remote loss of C_nH_{2n+2} or to the activation energy for fragmentation. There are several reasons for this. First, the precursor ion internal energy is not well-characterized. In addition, the results are dependent on the absolute detection limit of the instrument, the observation time of the instrument, the efficiency of conversion of kinetic energy into internal energy (which may vary with projectile and target masses), and the criteria used to determine the lowest center-of-mass collision energy at which loss of C_nH_{2n+2} occurs (e.g., how many members of the series must be observable). Estimation of an activation energy for charge-remote fragmentation from these threshold data also requires consideration of the possibility that the fragmentation could have a kinetic shift [53].*,** The lack of charge-remote fragmentation from some ions might be because different compounds have alternative charge-directed decomposition pathways which may compete to varying extents with charge-remote fragmentation and lead to competitive shifts [3,22,23] as well.

In summary, laboratory collision energies in the electronvolt range can promote charge-remote dissociation. While absolute values of the internal energy requirements for charge-remote fragmentation cannot reasonably be obtained from the data presented here, the relative values obtained for molecules of similar numbers of degrees of freedom and similar structures should be valid. These values indicate that the lowest center of mass collision energy at which charge-remote dissociation can be detected is compound dependent. Note that the problems described in the preceding paragraph also apply to high-energy collisional activation data on which previous estimates [12,13] of the activation energy for charge-remote fragmentation have been based. These estimates place the activation energy for charge-remote loss of C_nH_{2n+2} at less than 3 eV. In addition, one theoretical study resulted in a calculated activation energy of 4 eV for loss of C_nH_{2n+2} by the 1,4-hydrogen elimination mechanism; this value was decreased to 2.7 eV, based on the assumption that the MO calculation overestimated the activation energy to the same degree that it overestimated the activation energy for homolytic C–C cleavage [54]. These values are reasonable for a 1,4-hydrogen rearrangement. In our discussion of the mechanism below, we consider the possibility that mechanisms other than 1,4-hydrogen elimination contribute to charge-remote

---

* Rearrangement reactions, such as the one proposed for charge-remote fragmentation, have slowly rising $k(E)$ curves and the energy required to promote fragmentation at a rate fast enough for it to be observed on the time scale of the collisional activation experiment may be significantly higher than the activation energy for fragmentation.

**High energy requirements for fragmentation of molecules with large numbers of degrees of freedom have been suggested by several authors. For example, Russell and co-workers [16] have recently reported that they are unable to photodissociate dinitrophenyl derivatives of hexa- and heptapeptides by 3.5 eV photons although smaller dinitrophenyl peptides do produce detectable photofragment ions under the same conditions. Armentrout and co-workers [44] have encountered difficulties in measuring thresholds for dissociation of cluster ions containing more than six atoms; apparently there are significant kinetic shifts for dissociation of ions of this size.

fragmentation. The precursor ion internal energy and the competition between loss of C_nH_{2n+2} and other fragmentation pathways are considered first.

Influence of the precursor ion internal energy on the collisional activation spectra

As we mentioned above, the internal energy that an ion contains before it is mass-selected for collisional activation may influence the collisional activation mass spectrum. How great an effect the precursor ion internal energy can have on collisional activation spectra has been a source of controversy [47]. The factor that is of importance here is that ions with a large number of degrees of freedom can contain a significant amount of internal energy (thermal energy as well as energy deposited by the ionization method) and be stable to dissociation on the time scale of the ion source of a mass spectrometer (typically a few microseconds). One way to determine whether the mass-selected parent ions, which did not dissociate in the ion source, have a significant amount of internal energy is to vary this internal energy and establish its influence on the collision-activated dissociation spectra.

We illustrated in Figs. 1 and 2 that the method used to generate the ions of interest does in fact have a significant influence on the collisional activation spectra. The ratio of loss of C_nH_{2n+1} to loss of C_nH_{2n+2}, produced upon collisional activation of the selected ion, varies with the method used to produce the ions prior to their mass selection for collisional activation. The most likely explanation for these results is that the ions produced by CI and HP-FAB have lower internal energies than ions produced by standard FAB. This is consistent with the trends observed with an increase in collision energy or collision gas pressure.

As stated in the Introduction, the majority of high-energy collisional activation experiments on charge-remote fragmentation have been performed by using an electric sector scan to analyze the products. The spread of velocities of the daughter ions of each mass prevents unit mass resolution in these experiments (see Figs. 6b and 7). However, similar experiments performed by linked scan procedures to provide unit mass resolution show that ions corresponding to alkyl radical losses are also major products of kiloelectronvolt collisions for long chain functionalized alkane ions produced in a high-pressure chemical ionization source [17]. Certain radical ions (e.g., those produced by allylic cleavage) have also been observed in high-energy collisional activation spectra, obtained by linked scan procedures (four sector instrument), even when normal FAB was used to produce the ions [23]. These observations suggest that a greater percentage of radical ions is present in high-energy (kiloelectronvolt range) collisional activation spectra when CI is used to produce ions prior to mass selection than when FAB is used. This is consistent with our low-energy results (e.g., Fig. 1). Further experiments are needed to determine whether the extent of loss of C_nH_{2n+1} versus loss of C_nH_{2n+2}, upon high-energy collisional activation, varies with the method used to generate the ions.

It has already been illustrated in the Results section and directly above that loss of C_nH_{2n+1} occurs, under certain conditions, in addition to loss of C_nH_{2n+2}. Results obtained for a labelled compound, $[(CD_3)_3N(CD_2)_{13}CH_3]^+$, show that neither the loss of C_nH_{2n+1} nor the loss of C_nH_{2n+2} involves hydrogen scrambling between the remote alkyl terminus and the charge site (Fig. 3). Both series of losses ($-C_nH_{2n+1}$ and $-C_nH_{2n+2}$) are always observed with loss of all three hydrogens of the unlabelled terminal methyl group of the long alkyl chain. The absence of data indicating direct intervention of the charge site in the losses of C_nH_{2n+1} and C_nH_{2n+2} make it convenient to classify both series as charge-remote fragmentation, although the labelling data do not prove conclusively that the charge site plays no role in the losses of C_nH_{2n+2} and C_nH_{2n+1}.

Competition between other fragmentation pathways and loss of C_nH_{2n+2}

We showed above that the loss of C_nH_{2n+1} can occur at lower energies than the loss of C_nH_{2n+2} and that both of these pathways can be categorized as charge-remote fragmentation. In addition to these charge-remote processes, the compounds of Table 1 also undergo charge-directed fragmentation, i.e., fragmentation that directly involves the charge site of the ion. For ions of the type $CH_3(CH_2)_nX^+$, these processes include the formation of X^+ or XH^+ and the formation of alkyl ions, $C_nH_{2n+1}^+$. All of these different fragmentation types can compete with one another; the activation energies, relative rates of reaction, distribution of ion internal energies, and the time available for reaction all contribute to produce the spectrum that results upon collisional activation.

The major ion series present in either the high- [13] or low-energy collisional activation spectra of protonated alcohols or amines corresponds to the alkyl ion series, $C_nH_{2n+1}^+$ (e.g., see Figs. 4 and 8). Harrison and co-workers [37,38] have proposed for small amines that this series is initiated by dehydration or deamination, followed by further fragmentation of the initially formed alkyl ion. Deterding and Gross [13] have also suggested this general sequence of events from long-chain protonated carboxylic acids or esters (i.e., initial loss of water or an alcohol, followed by CO loss leading to an alkyl ion which then fragments further to produce an alkyl ion series). Our data indicate that the range of n values observed in the $C_nH_{2n+1}^+$ series varies with collision energy, and therefore with internal energy, in low-energy collisional activation of protonated alcohols and amines with the series extending to greater n values at lower collision energies. Even the ion corresponding to direct loss of NH_3 is detected following very low energy collisions (Fig. 4a).

Results from several types of experiment indicate that the collision energy required to produce detectable fragment ions corresponding to loss of C_nH_{2n+2} is higher than that required to produce observable alkyl ions. (i) The alkyl ion series dominates over the charge-remote ion series in both high- and low-energy collisional activation spectra. (ii) The alkyl ion series is present in metastable dissociation spectra of protonated amines (i.e., no collision gas present, same instrument as that used for high-energy collisions) while charge-remote fragmentation appears only with the addition of collision gas. (iii) In low-energy collisional activation experiments in a triple quadrupole instrument, the alkyl ion series from the protonated amines appears at lower collision energies than does the charge-remote series. (iv) In FTMS experiments the alkyl ion series is present upon collisional activation of protonated octadecylamine, but no charge-remote fragmentation is observed ($E_{\mathrm{max(lab)}} = 137\,\mathrm{eV}$, Xe target). Note that no information is gained from these experiments on the relative activation energies for the two processes. Since water is a better leaving group than ammonia, we suggest that the observation of charge-remote fragmentation from an amine is due to the fact that the higher activation energy expected for ammonia loss makes it possible for the charge-remote fragmentation to compete kinetically with ammonia loss, while the lower activation energy expected for dehydration from an alcohol makes competition from charge-remote fragmentation kinetically unlikely even at very high internal energies. This is supported, for example, by comparison of results obtained for octadecylammonium ion and trimethyloctadecylammonium ion. For trimethyloctadecylammonium ion, charge-remote fragmentation competes more effectively with alkyl ion formation than it does in the case of octadecylammonium ion (cf. Figs. 4b and 5d). This is consistent with the fact that $(CH_3)_3N$ is a poorer leaving group than NH_3. This proposal is compatible with suggestions that compounds with a stable (localized) site of charge undergo charge-remote fragmentation while compounds without a stable (localized) site of charge do not [13,55].

The data from both quadrupole and FTMS experiments suggest that the extent of charge-remote fragmentation correlates inversely with the energy required for cleavage at the charge site. For example, loss of a small neutral from the charge site of protonated 4-pentadecylpyridine is unlikely and charge-remote fragmentation occurs at relatively low internal energies for this compound [41], while loss of ammonia from protonated octadecylamine is a more facile process and charge-remote fragmentation from this compound requires much higher energies to compete. This is not to say that the activation energy for charge-remote fragmentation is different in the various types of compounds but rather that the alternative fragmentation pathways vary with compound type and lead to different competitive shifts for fragmentation.

Mechanistic information

A mechanism for a reaction describes, in detail, the series of elementary steps that make up the overall reaction; it is a working hypothesis to explain experimental data and is not necessarily unique even if it is consistent with all reported data. Many of the data reported for charge-remote loss of C_nH_{2n+2} are consistent with a 1,4-cyclic elimination mechanism. However, there are other results that cannot be explained by this mechanism; consequently, we consider here the possibility that alternative or additional mechanisms contribute to charge-remote fragmentation.

We illustrated that collision activation of $CH_3(CH_2)_nX^+$ results in the loss of alkyl radicals, $-C_nH_{2n+1}$, in addition to the loss of C_nH_{2n+2} (e.g., see Figs. 1–3) and that both of these losses may be classified as charge-remote fragmentation (see Fig. 3). High-energy collisional activation experiments, performed by linked scan procedures to provide unit mass resolution (on two [17] and four sector instruments [23]), show that alkyl radical losses also occur from compounds such as long-chain unsaturated fatty acids. In addition, it has been reported that the major charge-remote fragment ion series from perfluorinated compounds such as perfluorodecanesulfonate anion corresponds to loss of alkyl radicals, with ions corresponding to loss of C_nF_{2n+2} detected at much lower abundance [14]. Furthermore, we showed that the radical ions can undergo further fragmentation to form products that correspond to loss of C_nH_{2n+2} from the original parent ion (see reactions 2 and 3). These observations suggest that a radical mechanism is involved in charge-remote fragmentation. We showed earlier in this paper that the charge-remote losses of C_nH_{2n+1} units can occur at lower collision energies than do the losses of C_nH_{2n+2} units (see discussion of internal energy requirements and Figs. 3 and 4). One explanation for this observation is that the alkyl radical loss $(-C_nH_{2n+1})$ is the first step in a two-step mechanism and that ions corresponding to the first step (primary product ions) are detected only from low energy parent ions. Above a certain energy content, the primary fragment ion has enough energy to fragment further and only secondary ions are detected. This is consistent with our observation that these radical ions can undergo further fragmentation to form products that correspond to loss of C_nH_{2n+2} from the original parent ion. It is also consistent with the observation that the ratio of C_nH_{2n+2} loss to C_nH_{2n+1} loss increases with increasing precursor ion internal energy, with increasing laboratory collision energy, and with increasing collision gas pressure.

A radical mechanism that can explain both the loss of C_nH_{2n+1} and the loss of C_nH_{2n+2} is illustrated in reactions 4–7. An initial carbon–carbon bond cleavage (reaction 4), which should have approximately the same energy requirements for cleavage anywhere along an alkyl chain (approximately

3.8 eV) [1], is followed by loss of a hydrogen atom (requiring approximately 1.6 eV) [1] or ethylene units plus a hydrogen atom.

(4)

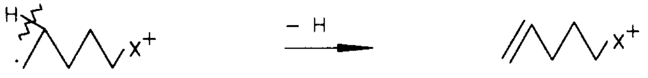

(5)

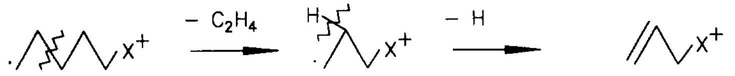

(6,7)

The energy requirement for the initial carbon–carbon bond cleavage is lowered substantially if the bond is only broken sufficiently to allow free relative rotation, but not separation, of the incipient fragments [56]. That is, if the species formed via the bond breaking has a lifetime sufficient to allow chemical reaction between the point of covalent bond breaking and the point of overcoming long-range attractive forces, the reaction will be considered to occur via an ion/molecule complex [56]. Chemistry (such as hydrogen transfers) would occur within this complex as illustrated by reactions 8–11.

(8)

(9)

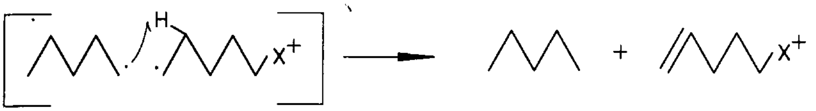

(10)

(11)

It is plausible that fragmentation of these large ions could involve an ion/neutral complex. For example, the formation of NH_4^+ from protonated octadecylamine (observed in both high- and low-energy collisional activation spectra) may occur via an alkyl-ion/ammonia complex (see Results section). An ion/molecule complex mechanism is attractive in that it would allow for formation of more types of product than either the simple consecutive direct-bond cleavage mechanism of reactions 4–7 or the 1,4-hydrogen elimination of reaction 1. This would help explain the complex clusters of peaks present in the spectra of many of the compounds of interest; peaks corresponding to losses other than C_nH_{2n+2} and C_nH_{2n+1} are often detected although they are of low relative abundance (e.g., loss of C_nH_{2n}, see Figs. 3 and 4 (inset)). Harrison and co-workers [57] have recently proposed that small protonated amines fragment by C_nH_{2n+2} loss via ion/molecule complexes. The extent to which an ion/molecule complex would contribute to the spectra of the compounds of Table 1 would depend on reaction conditions, especially the internal energy deposited and the time available for fragmentation. Note that any products formed via the ion/molecule complex (e.g., ions corresponding to alkane loss by H abstraction) would have to have lower internal energy requirements for formation than would products corresponding to complete separation (direct radical loss). Keep in mind that given enough excess internal energy, ions corresponding to direct radical loss could fragment further as illustrated in reactions 5–7. If the ion/molecule complex mechanism makes a major contribution to the product distribution, it is necessary to explain how reaction 10 could make a greater contribution than reaction 11 since this is observed experimentally for most reactants examined. One possibility is that the product distribution is governed by the relative stabilities of the radical ion and the radical. Another possibility is that the ion/molecule mechanism contributes to the product distribution, but does not dominate it.

For the loss of C_nH_{2n+2} by either the consecutive radical loss mechanism or the ion/molecule complex mechanism, the location of the unsaturation site in the final product will be determined by the rate of hydrogen loss or abstraction versus hydrogen rearrangement. If the hydrogen atom loss occurs before any hydrogen rearrangements, the final product will be a terminally unsaturated ion. Very little information is available on the structure of the products of charge-remote fragmentation. Our data in reactions 2 and 3 could be consistent with formation of a terminally unsaturated ion. A published spectrum of a product ion (*m/z* 197) produced by charge-remote fragmentation of the $[M + 2Li–H]^+$ ion of hydroxyricinelaidic acid, is similar to the spectrum of authentic $[M + 2Li–H]^+$ ions of 10-undecenoic acid. Data for the *m/z* 93 ion from pentadecylpyridine suggests that it may have the structure of a distonic radical ion [35]. Further work is required to determine the structures of both the neutral and ionic products of charge-remote fragmentation under given reaction conditions.

A radical mechanism can be used to explain many features of charge-remote fragmentation spectra that cannot be explained by a 1,4-hydrogen rearrangement. Three processes accounted for by a radical mechanism include the loss of CH_4, the formation of odd-electron product ions, and enhanced allylic cleavage from unsaturated ions. The loss of CH_4 by a radical mechanism such as that shown in reactions 4 and 5 or 8 and 10 would occur similarly to all other losses of C_nH_{2n+2} by the mechanism. Many of the reported variations [7,9–11,13] in fragmentation patterns that occur when substituent or unsaturation sites are introduced into molecules are consistent with involvement of a radical mechanism because they can be explained by consideration of relative radical stabilities. For example, the enhanced relative abundance of peaks corresponding to charge-remote allylic cleavage could be due to the greater stability of allylic radicals versus primary radicals. Similar arguments can be posed to explain enhanced cleavage at substituent sites: secondary radicals are more stable than primary radicals. For the alternative cyclic rearrangement mechanism, unusual steric effects seem to be the most reasonable explanation for enhanced allylic cleavage or enhanced cleavage beta to a substituent site. However, this explanation is difficult to reconcile with the facts that *cis* and *trans* isomers of alkenes have been reported to give virtually identical fragmentation patterns [9] and that allylic cleavage by a cyclic rearrangement mechanism would require (i) an energetically unfavorable abstraction of a vinylic hydrogen, or (ii) the introduction of a 1,4-conjugate elimination reaction and a retroene reaction on alternate sides of the double bond [6].

The suggestion that a radical mechanism plays a role in charge-remote fragmentation is also consistent with kinetic evidence provided by the results presented in this paper and in the literature (e.g., see data in refs. 7 and 13). That is, the energetics of dissociation for fragmentation pathways that occur in lieu of, or at lower energies than, charge-remote fragmentation can provide mechanistic information on charge-remote fragmentation. For example, charge-directed formation of an alkyl ion series ($C_nH_{2n+1}^+$) often requires lower energies to be detected than do charge-remote losses of C_nH_{2n+1} and C_nH_{2n+2} to produce a radical ion series and the unsaturated ion series ($(C_nH_{2n-1})X^+$), respectively (see Figs. 1–3). As stated previously, the alkyl ions (43^+, 57^+, 71^+, 85^+...) are thought to form by an initial charge-directed loss of X from $CH_3(CH_2)_nX^+$ where X = H_2O, NH_3, $N(CH_3)_3$, etc. If this charge-directed fragmentation involves a direct bond cleavage reaction, then a charge-remote fragmentation involving a rate-determining direct bond cleavage would compete more effectively with the charge-directed dissociation as the internal energy of the ions is increased than would a charge-remote fragmentation involving a rate determining rearrangement reaction. This is because the rate constant for a rearrangement generally rises more slowly with increasing internal energy than do the rate constants for direct bond cleavages [3,5,53].

TABLE 2

Fragment ion spectra predicted by Boltzmann distributions for tetramethylammonium ion

	Ion abundance (%)	
	1500 K	2400 K
M − CH_4	21	1
M − CH_3	77	30
M − CH_3 − H	2	69

We stress here that more than one mechanism for charge-remote fragmentation may be operative and that the mechanisms may occur to varying degrees depending on the reaction conditions. For example, the possibility can be entertained for some ions that the direct radical mechanism (reactions 4–7), the ion/molecule mechanism (reactions 8–11), and the 1,4-hydrogen rearrangement (reaction 1) contribute to charge-remote fragmentation. The rearrangement mechanism would be expected to dominate at low internal energies while the radical mechanism would be preferred at higher energies. The ion/molecule mechanism would play a role only over a narrow low internal energy range [55]. It is instructive to consider competition of a radical mechanism and a rearrangement mechanism for the fragmentation of a simple ion, tetramethylammonium ion, which loses CH_4 by a rearrangement reaction and by loss of CH_3 followed by loss of H. The relative rates of dissociation and the calculated breakdown curve for dissociation illustrate that the rearrangement reaction is favored only from ions of low internal energies (see ref. 5a, pp. 54–59). The corresponding fragment ion spectra predicted by Boltzmann distributions characterized by temperatures of 1500 K and 2400 K are given in Table 2, where M is tetramethylammonium ion. This example illustrates that the relative contribution from each pathway can vary significantly with internal energy. A similar situation could apply to charge-remote losses of C_nH_{2n+1} and C_nH_{2n+2} with a contribution also expected from the ion/molecule complex mechanism.

SUMMARY

The data presented above indicate that (i) charge-remote loss of C_nH_{2n+2} can be observed upon low-energy collision-activated dissociation, with the heavier target gas Xe illustrated to be much more effective than Ar in promoting charge-remote fragmentation of the compounds examined here, (ii) ions produced by FAB contain a significant amount of internal energy which influences the relative abundance of charge-remote fragment ions produced by electronvolt collisional activation, (iii) the losses of C_nH_{2n+1} and C_nH_{2n+2}

(for an unlabelled compound) occur from $[(CD_3)_3N(CD_2)_{13}CH_3]^+$ with no apparent hydrogen/deuterium scrambling, and (iv) the collision energy required for observation of charge-remote fragmentation varies with the compound studied. A reasonable explanation for the differences in fragmentation patterns observed for different compounds is that competitive shifts occur. The magnitude of these shifts will vary with the types of competitive dissociation "introduced" by various functional groups and will depend on the activation energies and rates of the alternative pathways relative to those for loss of C_nH_{2n+2}. That is, while the charge site may not be directly involved in charge-remote fragmentation, the type of functional group present determines the overall spectrum and, in some instances, can significantly reduce or prevent charge-remote loss of C_nH_{2n+2}. The data show that a radical mechanism may be involved in charge-remote fragmentation.

EXPERIMENTAL

The low-energy gas-phase data were obtained with a triple quadrupole instrument (Finnigan-MAT TSQ-70). Ions were generated by FAB (8 keV Xe beam; *m*-nitrobenzylalcohol or glycerol matrix) or CI (isobutane). The collision-activated dissociation spectra were obtained at laboratory collision energies ranging from 5 to 195 eV with Ar or Xe as the collision target. The collision gas pressure was monitored by a capacitance manometer (MKS Baratron) connected to the collision chamber. For low pressure conditions the collision gas pressure was 0.07 mTorr; this corresponds to single-collision conditions for dissociation of the *m/z* 219 ion from perfluorotributylamine (based on a linear increase in daughter ion abundances as a function of collision gas pressure) [58]. For multiple-collision conditions, 0.2–1.5 mTorr argon was used. The offset voltage of the third quadrupole was ramped with mass such that all daughter ions enter the quadrupole with approximately 5–6 eV kinetic energy. This ramp was made with the assumption that the fragment ions have 90% of their expected kinetic energy based on the collision energy of the parent ion and the ratio of the parent and daughter masses. In this triple quadrupole instrument, the r.f. applied to the second quadrupole is a variable fraction of that applied to the first quadrupole. The default value of the Mathieu parameter, q, in the second quadrupole is 0.2.

High-energy collisional activation experiments were performed with a reverse-geometry (BE) instrument (VG ZAB-2F). Ions were generated by fast-atom bombardment (8 keV Xe) using neat samples or samples dissolved in *m*-nitrobenzyl alcohol. The $[M + Li]^+$ ion of oleyl alcohol was produced by the addition of lithium nitrate, rather than lithium iodide, to neat oleyl alcohol in order to avoid formation and fragmentation of $Li_3I_2^+$, which has the same nominal mass as lithiated oleyl alcohol. Collisions of mass-selected, 8 keV ions with helium target gas yielded high-energy collision-activated dissociation spectra. The pressure in the collision cell was adjusted to reduce the main beam intensity by approximately 50% and corresponded to a pressure reading in the 10^{-7} Torr range (measured by an ion gauge situated outside the collision cell).

Angle-resolved (ARMS) and MS–MS–MS experiments were carried out on a mass spectrometer (Finnigan-MAT 8200) modified by the addition of an r.f.-only quadrupole collision cell and a mass-analyzing quadrupole [59]. Ions were produced by chemical ionization. For the ARMS experiments, the scattering angle was selected by electrical deflection of the ion beam along the *xz* plane as it leaves the ion source and prior to entering the first field-free region collision cell. Collision-induced dissociation product ions are transmitted through the analyzers only when scattered through an angle identical to that through which they were initially deflected. The main beam was attenuated by ca. 50%. Fragment ions generated by 3 keV collisions with Ar and scattered at selected angles in the range 0–2.5° were analyzed by using a linked scan of the sector analyzers. For MS–MS–MS experiments, a particular fragment ion produced by 3 keV collisions with Ar was selected with a linked scan of the sectors, decelerated to 80 eV and allowed to collide with Xe. Products of the low-energy collisions were analyzed by the final quadrupole.

ACKNOWLEDGEMENTS

We thank R.G. Cooks, S.R. Horning and M. Vincenti for MS–MS–MS and angle-resolved mass spectrometry data and R.G. Cooks and H.I. Kenttamaa for many helpful discussions. We thank S. McElvany for the FTMS data, G. Mushrush for supplying the 2- and 4-pentadecylpyridine samples [60], and Al Tuinman and L.J. Magid for the $[(CD_3)_3N(CD_2)_{13}CH_3]^+$ [39]. V.H.W. acknowledges the National Research Council and the Naval Research Laboratory for a cooperative postdoctoral research associateship.

REFERENCES

1 W. Forst, Theory of Unimolecular Reactions, Academic, New York, 1973.

2 R.G. Cooks, Collision Spectroscopy, Plenum, New York, 1978.

3 K. Levsen, Fundamental Aspects of Organic Mass Spectrometry, Verlag Chemie, Weinheim, 1978.

4 F.W. McLafferty, Interpretation of Mass Spectra, 3rd edn., University Science, Mill Valley, CA, 1980.

5 (a) K.L. Busch, G.L. Glish and S.A. McLuckey, Mass Spectrometry/Mass Spectrometry, VCH, New York, 1988.
(b) F.W. McLafferty (Ed.), Tandem Mass Spectrometry, Wiley, New York, 1983.

6 J. Adams, Mass Spectrom. Rev., 9 (1990) 141.
7 N.J. Jensen, K.B. Tomer and M.L. Gross, J. Am. Chem. Soc., 107 (1985) 1863.
8 J. Adams and M.L. Gross, J. Am. Chem. Soc., 111 (1989) 435.
9 K.B. Tomer, F.W. Crow and M.L. Gross, J. Am. Chem. Soc., 105 (1983) 5487.
10 K.B. Tomer, N.J. Jensen and M.L. Gross, Anal. Chem., 58 (1986) 2429.
11 D.A. McCrery, D.A. Peake and M.L. Gross, Anal. Chem., 57 (1985) 1181.
12 J. Adams and M.L. Gross, J. Am. Chem. Soc., 108 (1986) 6915.
13 L.J. Deterding and M.L. Gross, Org. Mass Spectrom., 23 (1988) 169.
14 P.A. Lyon, K.B. Tomer and M.L. Gross, Anal. Chem., 57 (1985) 2984.
15 L.M. Mallis and D.H. Russell, Anal. Chem., 58 (1986) 1076.
16 R.E. Tecklenburg, Jr., M.N. Miller and D.H. Russell, J. Am. Chem. Soc., 111 (1989) 1161.
17 A.M. Bambagiotti, S.A. Coran, F.F. Vincieri, T. Petrucciani and P. Traldi, Org. Mass Spectrom., 21 (1986) 485.
18 A.J. Alexander, P. Thibault and R.K. Boyd, Rapid Commun. Mass Spectrom., 3 (1989) 30.
19 F.W. Rollgen, F. Borchers, U. Giessman and K. Levsen, Org. Mass Spectrom., 12 (1977) 541.
20 R. Weber, K. Levsen, A.J.H. Boerboom and J. Haverkamp, Int. J. Mass Spectrom. Ion Phys., 46 (1983) 305.
21 R.S. Johnson, S.A. Martin and K. Biemann, Int. J. Mass Spectrom. Ion Processes, 86 (1988) 137.
22 V.H. Wysocki, M.E. Bier and R.G. Cooks, Org. Mass Spectrom., 23 (1988) 627.
23 K.B. Tomer, Org. Mass Spectrom., 24 (1989) 969.
24 M.S. Kim and F.W. McLafferty, J. Am. Chem. Soc., 100 (1978) 3279.
25 M. Labrenovic, J.H. Beynon, S.H. Lee and M.S. Kim, Int. J. Mass Spectrom. Ion Processes, 65 (1985) 197.
26 F.W. McLafferty, P.F. Bente III, R. Kornfeld, S.-C. Tsai and I. Howe, J. Am. Chem. Soc., 95 (1973) 2120.
27 V.W. Wysocki, H.I. Kenttämaa and R.G. Cooks, Int. J. Mass Spectrom. Ion Processes, 75 (1987) 181.
28 S. Chowdhury and A.G. Harrison, J. Am. Chem. Soc., 110 (1988) 7345.
29 D.F. Fraley and D.L. Lawrence, Proc. 33rd ASMS Conf. Mass Spectrometry and Allied Topics, San Diego, CA, 1985, pp. 144–145.
30 V.H. Wysocki, M.M. Ross, S.R. Horning and R.G. Cooks, Rapid Commun. Mass Spectrom., 2 (1988) 214.
31 A.G. Harrison, Chemical Ionization Mass Spectrometry, CRC Press, Boca Raton, FL, 1983.
32 C. Fenselau and R.J. Cotter, Chem. Rev., 87 (1987) 501.
33 J.H. Callahan, R.J. Colton and M.M. Ross, Int. J. Mass Spectrom. Ion Processes, 90 (1989) 9.
34 S. Hammerum, Mass Spectrom. Rev., 7 (1988) 123.
35 V.H. Wysocki and H.I. Kenttämaa, J. Am. Chem. Soc., 112 (1990) 5110.
36 A.A. Tuinman and K.D. Cook, Rapid Commun. Mass Spectrom., 3 (1989) 289.
37 E.J. Reiner, R.A. Poirier, M.R. Peterson, I.G. Csizmadia and A.G. Harrison, Can. J. Chem., 64 (1986) 1652.
38 E.J. Reiner and A.G. Harrison, Org. Mass Spectrom., 19 (1984) 343.
39 A.A. Tuinman, K.D. Cook and L.J. Magid, J. Am. Soc. Mass Spectrom., 1 (1990) 85.
40 B.S. Freiser, in M. Farrar and W.H. Saunders Jr. (Eds.), Techniques for the Study of Ion/Molecule Reactions, Wiley, New York, 1988, Chap. 11.
41 R.B. Cody, Rapid Commun. Mass Spectrom., 2 (1988) 260.

42 M.S. Lee and R.A. Yost, Biomed. Environ. Mass Spectrom., 15 (1988) 193.

43 K.L. Schey, H.I. Kenttämaa, V.H. Wysocki and R.G. Cooks, Int. J. Mass Spectrom. Ion Processes, 90 (1989) 71.

44 S.K. Loh, D.A. Hales, L. Lian and P.B. Armentrout, J. Chem. Phys., 90 (1989) 5466.

45 H.I. Kenttämaa, Org. Mass Spectrom., 20 (1985) 703.

46 P. Lyon, F.W. Crow, K.B. Tomer and M.L. Gross, Anal. Chem., 56 (1984) 2278.

47 J.L. Holmes, Org. Mass Spectrom., 20 (1985) 169.

48 D.E. Giblin, Proc. 33rd ASMS Conf. Mass Spectrometry and Allied Topics, San Diego, CA, 1985, p. 921.

49 P.A. van Koppen, A.J. Illies, S. Liu and M.T. Bowers, Org. Mass Spectrom., 17 (1982) 399.

50 (a) G.A. Junk and H.J. Svec, Z. Naturforsch., Teil B, 23 (1968) 1; D.R. Bidinosti and N.S. McIntyre, Can. J. Chem., 45 (1967) 641.
(b) A. Foffani and S. Pignataro, Z. Phys. Chem. (Frankfurt am Main), 45 (1969) 79.
(c) M.R. Litzow and T.R. Spalding, Mass Spectrometry of Inorganic and Organo-Metallic Compounds, Elsevier, Amsterdam, 1973, pp. 475–490.

51 T.F. Magnera, D.E. David, D. Stulik, R.G. Orth, H.T. Jonkman and J. Michl., J. Am. Chem. Soc., 111 (1989) 5036.

52 P.J. Chantry, J. Chem. Phys., 55 (1971) 2746.

53 C. Lifshitz, Mass Spectrom. Rev., 1 (1982) 309.

54 M.M. Siegel and N.B. Colthup, Appl. Spectrosc., 42 (1988) 1214.

55 M.L. Gross, Mass Spectrom. Rev., 8 (1989) 165.

56 D.J. McAdoo, Mass Spectrom. Rev., 7 (1988) 363.

57 E.J. Reiner, A.G. Harrison and R.D. Bowen, Can. J. Chem., 67 (1989) 2081.

58 J.A. Nystrom, M.M. Bursey and J.R. Hass, Int. J. Mass Spectrom. Ion Processes, 55 (1984) 263.

59 S.R. Horning, M. Vincenti and R.G. Cooks, J. Am. Chem. Soc., 112 (1990) 119.

60 D.R. Hardy, G.W. Mushrush, W.M. Stalick, E.J. Beal and R.N. Hazlett, Rapid Commun. Mass Spectrom., 2 (1988) 16.